Available online at www.sciencedirect.com
ScienceDirect
Cement and Concrete Research 37 (2007) 815–822
Cement and Concrete Research

Properties and hydration of blended cements with steelmaking slag

S. Kourounis [a], S. Tsivilis [a,*], P.E. Tsakiridis [b], G.D. Papadimitriou [b], Z. Tsibouki [c]

[a] National Technical University of Athens, School of Chemical Engineering, Laboratory of Analytical and Inorganic Chemistry, 9 Heroon Polytechniou St, 15773 Athens, Greece
[b] National Technical University of Athens, School of Mining and Metallurgical Engineering, Laboratory of Physical Metallurgy, 9 Heroon Polytechniou St, 15780 Athens, Greece
[c] Hellenic Cement Research Center Ltd, Heracles Group, 15 K. Pateli, 14123, Lykovrissi, Athens, Greece

Received 17 December 2005; accepted 9 March 2007

Abstract

The present research study investigates the properties and hydration of blended cements with steelmaking slag, a by-product of the conversion process of iron to steel. For this purpose, a reference sample and three cements containing up to 45% w/w steel slag were tested. The steel slag fraction used was the "0–5 mm", due to its high content in calcium silicate phases. Initial and final setting time, standard consistency, flow of normal mortar, autoclave expansion and compressive strength at 2, 7, 28 and 90 days were measured. The hydrated products were identified by X-ray diffraction while the non-evaporable water was determined by TGA. The microstructure of the hardened cement pastes and their morphological characteristics were examined by scanning electron microscopy. It is concluded that slag can be used in the production of composite cements of the strength classes 42.5 and 32.5 of EN 197-1. In addition, the slag cements present satisfactory physical properties. The steel slag slows down the hydration of the blended cements, due to the morphology of contained C_2S and its low content in calcium silicates.

Keywords: Steelmaking slag; Blended cements (D); Physical properties (C); Mechanical properties (C); Hydration (A)

1. Introduction

At the present, most industrial slags are being used without taking full advantage of their properties or disposed rather than used. The main kinds of metallurgical slags are properly fast cooled iron blast furnace slag (ggbs), steel slag, phosphorus slag, copper slag and lead slag. Due to their chemical and mineral composition, these slags have cementitious and/or pozzolanic properties and can be potentially used as cement main constituents. Today, most metallurgical slags are used as aggregates for different applications, and only the ground granulated blast furnace slag is used for a partial Portland cement replacement [1].

Iron blast furnace slag is formed in the process of pig iron manufacture from iron ore. Ggbs results from the fast cooling of the molten slag and is a pozzolanic as well as a latent hydraulic material. Ggbs has been extensively studied as a cement or concrete constituent and as an alkali activated cementitious material [2–7].

Steel slag is the industrial waste resulting from the steel-refining process in a conversion furnace. Fifty million tons per year of steel slag is produced worldwide, while nearly 12 million tons of steel slag is the annual production in Europe [8]. Owing to the intensive research work during the last 30 years, about 65% of the produced steel slag is used today on qualified fields of applications. But the remaining 35% of this slag is still dumped [9]. Further intensive research work is needed in order to decrease this rate as far as possible.

Two different approaches exist for the incorporation of steel slag in cement production. The first one involves the use of slag, mixed with limestone and clay, as raw material feed to the cement kiln [10]. This may be a solution to the disposal problem but there is not any energy benefit (the slag must be clinkered) or economic benefit (one inexpensive material is substituted for another). A more attractive approach is the incorporation of steel slag in cement.

* Corresponding author. Tel.: +30 2107723262; fax: +30 2107723188.
E-mail address: stsiv@central.ntua.gr (S. Tsivilis).

0008-8846/$ - see front matter © 2007 Elsevier Ltd. All rights reserved.
doi:10.1016/j.cemconres.2007.03.008

As the chemical composition of steel slag is highly variable, the mineral composition of steel slag also varies. Olivine, merwinite, C_3S, C_2S, C_4AF, C_2F, RO phase (CaOFeO–MnO–MgO solid solution) and free-CaO are common minerals in steel slag. Its chemical composition consists of CaO 45–60%, SiO_2 10–15%, Al_2O_3 1–5%, Fe_2O_3 3–9%, FeO 7–20%, MgO 3–13%, and P_2O_5 1–4% [1]. The presence of C_3S, C_2S, C_4AF and C_2F endorses steel slag hydraulic properties. However, the C_3S content in steel slag is much lower than that in Portland cement. Thus, steel slag can be regarded as a low strength hydraulic material.

Although the use of ggbs in cement and concrete technology has been extensively discussed, few papers have been published on the incorporation of steel slag in composite cements [1,8,9,11–14]. The main reasons for this are the highly variable composition of the slag (each slag must be considered as a case study), the low content of reactive calcium silicate compounds and the high content of free calcium and magnesium oxides that may cause volume expansion problems. However, a special steel slag cement, which is composed mainly of steel slag, blast furnace slag and Portland cement, has been commercially marketed in China, absorbing approximately 40% of the total steel slag production [11].

The aim of the present research work is to investigate the possibility of using the steel slag from the Hellenic steel industry as a constituent in composite cements. Instead of the steel slag as it is, the authors studied the use of the "0–5 mm" fraction. This fraction is enriched in hydraulic calcium silicate phases and this is expected to improve the reactivity of slag. One reference cement and three cements containing up to 45% w/w steelmaking slag were prepared. Water demand, setting time, soundness and compressive strength were measured. In addition, XRD, TGA and SEM were applied in order to study the hydration products, the hydration rate and the microstructure of the cement-slag system.

2. Experimental

Steelmaking slag supplied from Sidenor Steel Products Manufacturing Company S.A. of Greece was added to Portland cement (CEM I 42.5) produced by Heracles General Cement Company of Greece. The steel slag was crushed in a jaw crusher and the fraction used in this study was the "0–5 mm". Preliminary examination had showed that this fraction presented high content in calcium silicate phases and small amounts of metallic iron. The chemical composition and the physical characteristics of the steel slag and the cement used are listed in Table 1. The mineralogical phases of CEM I 42.5 and slag, which were determined by XRD analysis, using a Siemens D5000 diffractometer with nickel-filtered $CuK\alpha_1$ radiation (=1.5405 Å, 40 kV and 30 mA), are given in Figs. 1 and 2.

The steel slag microstructure was examined by optical microscopy. The microscopic observation of the polished impregnated samples was achieved using a Jenapol optical microscope in reflected light.

Prior to the preparation of the blends with cement, the steel slag (size fraction: 0–5 mm) was ground, in a 1 kg laboratory ball mill using steel balls as grinding medium, to a specific surface area of about 3000 cm^2/g (according to the Blaine air permeability method) [15]. Then, the blended cements were produced by mixing the slag and the cement. The mixing ratios, as well as the physical characteristics of the cements are given in Table 2.

The standard consistency and setting time of cement pastes were determined using a Vicat apparatus according to the European Standard EN 196-3 [16]. The determination of the normal mortar flow was carried out according to ASTM C1437 [17]. The soundness test was performed according to standard test method for autoclave expansion of Portland cement (ASTM C151) [18]. Compressive strength measurements were conducted at the ages of 2, 7, 28 and 90 days on mortar prisms (dimensions 40×40×160 mm), prepared and tested in accordance with European Standard EN 196-1 [19].

For the study of the hydration products, the cement pastes were prepared by mixing 300 g of mixtures with 75 ml of water. Then, they were cured in tap water at a temperature 20± 2 °C. At the ages of 1, 2, 7, 28 and 90 days, the hydration was stopped by means of acetone and ether extraction.

The hydration products were mineralogically determined by X-ray diffraction. XRD measurements were conducted with a Siemens D5000 diffractometer using nickel-filtered $CuK\alpha_1$ radiation (=1.5405 Å), 40 kV voltage and 30 mA current. TGA/DTA was used for the evaluation of the hydration rate. A Mettler–Toledo TGA/SDTA 851 instrument was used. Type R thermocouple (Pt-13% Rh/Pt) was used for temperature measurements in this instrument. The samples were taken in a ceramic crucible and heated from room temperature to 900 °C at a constant rate of 10 °C/min in an atmosphere of carbon dioxide free nitrogen, flowing at 50 cm^3/min. TGA/DTA were carried out simultaneously. Finally, in order to get an idea of their morphology, the hydration products were also examined by scanning electron microscopy (SEM) using a Jeol 6100 Scanning Electron Microscope. Experimental conditions

Table 1
Chemical analysis and physical characteristics of cement and steel slag used

Oxides	Chemical analysis (%)	
	CEM I-42.5	Steel slag
SiO_2	21.12	17.53
Al_2O_3	5.55	6.25
Fe_2O_3	1.92	26.36
CaO	63.80	35.70
MgO	2.25	6.45
K_2O	1.03	0.26
Na_2O	0.25	0.20
SO_3	3.04	0.75
MnO	–	2.50
TiO_2	0.15	0.76
ZnO	–	0.85
Free CaO	1.15	–
LOI	0.85	2.24
Physical characteristics		
Specific surface (cm^2/g)	3850	3070
Specific gravity (g/cm^3)	3.16	3.77

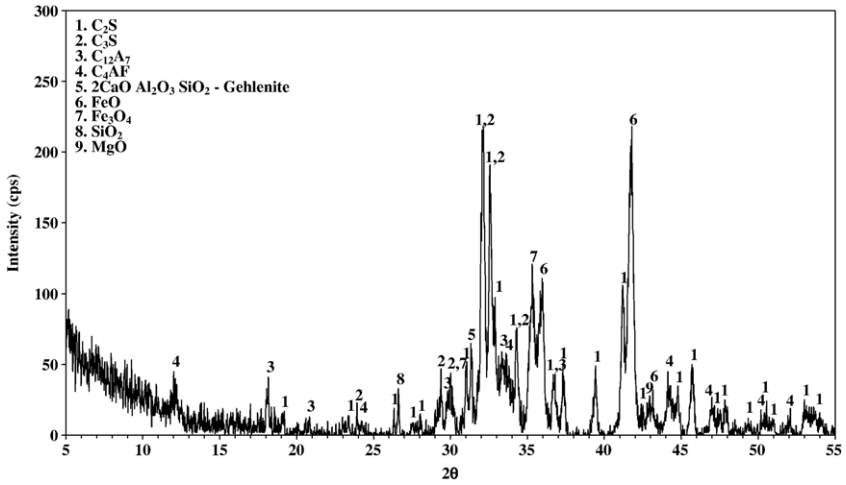

Fig. 1. X-ray diffraction of steel slag used.

involved 20 kV accelerating voltage. Microanalysis of the cement pastes was performed by a Noran TS 5500 Energy Dispersive Spectrometer (EDS) connected to the SEM.

3. Results and discussion

3.1. Chemical, physical and mineralogical characteristics of the materials

As shown in Table 1, the main oxides of steel slag fraction used are CaO, Fe_2O_3, SiO_2, MgO and Al_2O_3. Like most metallurgical slags, it has a chemical composition similar to that of Portland cement. However, there are significant differences in the mineralogical phases present in these two materials (Figs. 1 and 2). The main difference in steel slag is the high iron oxide content, which exists in both the di-and trivalent states. Fig. 1 indicates that although crystalline calcium silicates are present in steel slag, the absence of a strong tricalcium silicate peak at 29.2° 2θ and 51.5° 2θ indicates a deficiency in alite, which is the primary strength contributing phase during Portland cement hydration. Moreover, it should be noticed that wustite (FeO), which is the predominant mineral phase in steel slag, does not occur in pure cement. This phase has no cementitious properties and does not combine to form hydraulic phases [13]. X-ray diffraction confirmed the absence of γ-C_2S. Dicalcium silicate was detected as β-C_2S, which has been probably stabilized in presence of impurities (Fe^{3+}, Al^{3+} ions). The detection of C_4AF, which is one of the major mineral phases found in Portland cement, indicates that the trivalent iron was able to combine with calcium oxide and alumina to produce the ferrite phase upon cooling from the melt.

The above conclusions were also confirmed by optical microscopy observations (Fig. 3). Although the coarse alloy and metal oxide particles have been separated and recovered, the steel slag still contains small amounts of metallic Fe. The presence of finger C_2S was attributed to the slow rate of cooling. This fact was attested also by the absence of amorphous glass between 26° 2θ and 36° 2θ. The liquid phase occurred as uniformly distributed large crystals. The ferrite phase exhibits a dendritic, prismatic and massive form.

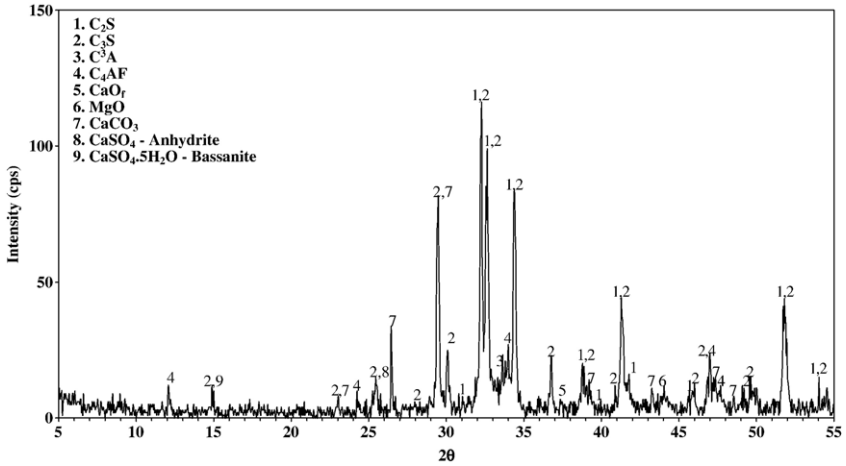

Fig. 2. X-ray diffraction of cement used.

Table 2
Composition and characteristics of tested cements

Code	CEM I 42.5 (w/w %)	Steel slag (w/w %)	Specific surface area (cm^2/g)	Specific gravity (g/cm^3)
C1	100	0	3850	3.16
C2	85	15	3730	3.24
C3	70	30	3620	3.32
C4	55	45	3500	3.41

Table 3
Physical properties of tested cements

Sample	Steel slag (% w/w)	Water demand (% w/w)	Setting time (min)		Autoclave expansion (%)	Flow of normal mortar (%)
			Initial	Final		
C1	–	27.0	155	185	−0.04	103.0
C2	15	26.0	170	210	−0.02	108.5
C3	30	25.0	210	240	−0.20	111.5
C4	45	23.5	220	260	0.33	113.5

3.2. Physical and mechanical properties of blended cements

Table 3 presents the cement water demand, the setting time and the normal mortar flow of the tested samples. The "water demand" is generally considered to be the quantity of water required for the preparation of a cement paste with standard consistency, as specified in EN 196-3. The slag containing cements demand less water than the reference pure cement. The water demand is less, the higher the slag content of the cement. The decreased water demand is attributed to the delayed hydration of the slag, due to its mineralogical composition. The flow tests confirm the above results and show that the slag addition improves the mortar workability. The replacement of cement with slag, which is less reactive than pure cement, reduces the amount of ettringite formed during the early hydration thus resulting to higher workability of the mortar [3].

The blended cements showed longer setting times than the pure cement. This is expected as the increase of steel slag content reduces the cement content in the mix (cement dilution effect). As a result, hydration process slows down causing setting time to increase. The longer setting time of slag cements has also been reported by other authors and has been associated with the low Al_2O_3 content and/or high MgO and MnO_2 content in the slag. It must be noted that this particular slag has lower MgO and MnO_2 content and higher Al_2O_3 content in comparison with others mentioned in the literature and this seems to be the reason for the less pronounced setting delay [8,20]. In any case, the low hydration rate is an advantage for certain applications, since it means low rate of heat evolution, a fact that is of great importance in mass concrete constructions.

The results of the autoclave expansion are presented in Table 3. In the case of cements containing 15% and 30% slag, the changes in length of the test specimens are high enough, but they satisfy the standard requirements of ASTM C 151 (max autoclave expansion: 0.8%).

Fig. 4 shows the compressive strength development of slag cements in relation to the cement replacement level. It is observed that slag cements develop lower strength, at all ages, compared to reference cement. The strength decrease is higher, the higher the slag content. The results in Fig. 4 confirm that cements containing 15% or 30% slag satisfy the requirements of the strength class 42.5 of EN 197-1, while the cement containing 45% slag satisfies the requirements of the strength class 32.5 of EN 197-1.

Fig. 5 presents the relative strength of tested cements in relation to curing age and replacement level. Relative strength is the ratio of the strength of the slag cement to the strength of the reference cement at each particular curing time. The rate of strength development of reference cement depends mainly on its hydration rate, while in cement-slag systems it also depends on the hydration and the latent hydraulic reactions of slag. Therefore, the relative strength-time plots provide an insight into the rates of reaction in the blended system relative to the pure cement. Fig. 5 shows that at 7 days the slag cements present a compressive strength that equals the 82%, 63% and 46% of the reference cement strength for 15%, 30% and 45% slag content respectively. At 90 days the slag cements present a compressive strength that equals the 92%, 81% and 59% of the

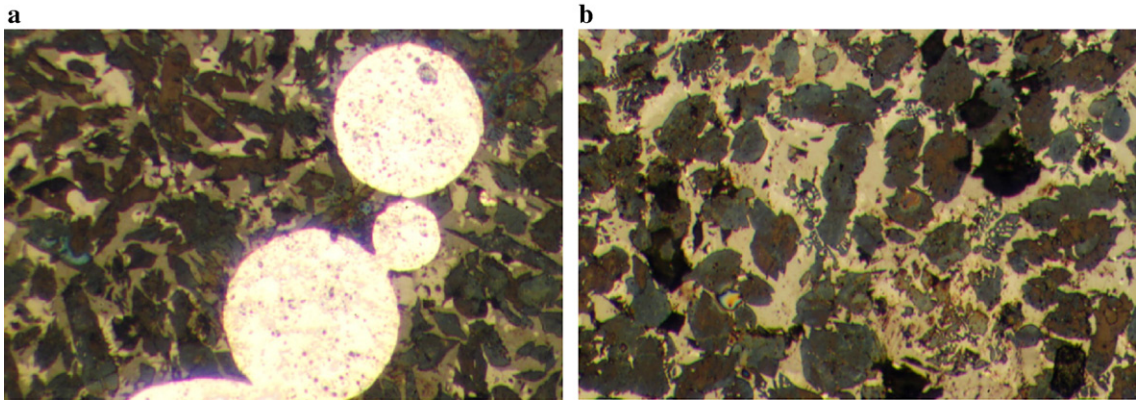

Fig. 3. Microstructure of steel slag used (a: finger C_2S and skeletal C_3S due to slow cooling (×500), b: entrapped metallic Fe and anhedral C_3S with decomposition (×200)).

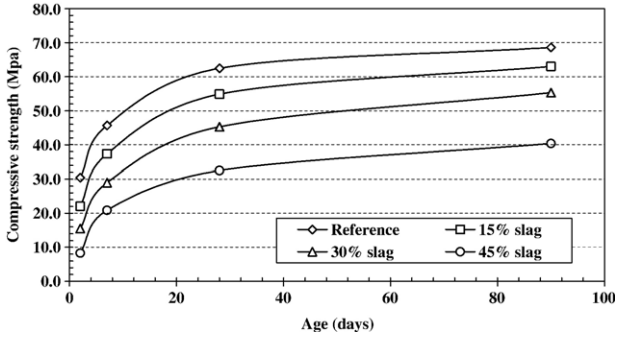

Fig. 4. Strength development of the cements.

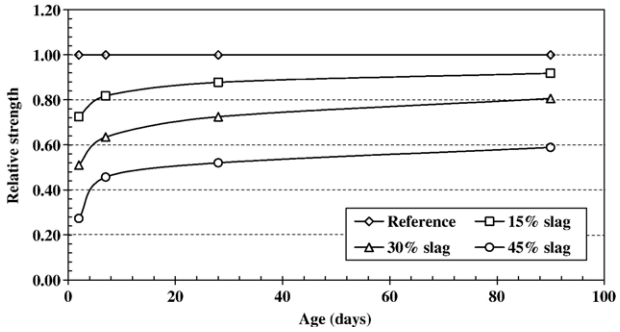

Fig. 5. Relative strength of slag cements in relation to curing age and replacement level (relative strength: ratio of the strength of slag cement to the strength of reference cement).

reference cement strength for 15%, 30% and 45% slag content respectively. At early ages, the strength development is mainly affected by the pure cement hydration and the slag presence seems to occlude this process. At longer ages the strength development is affected by the hydration as well as the hydraulic reactions of the slag. The delayed contribution of the slag on the cement strength is attributed to the crystal size and structure of C_2S contained in slag. It has a crystal size greater than 70 μm and it is characterized by clusters with finger structure with no well formed rounded crystals.

The lower compressive strength of cements containing steel slag has also been observed by other authors and it has been attributed to the fact that the C3S content in steel slag is much lower than in Portland cement [1,8,20].

Altun and Yılmaz [8] have reported that blended cements containing 15–30% steel slag develop the 66–83% of the pure cement's strength at 28 days. In this study, it is found that the cements with the same level of replacement have developed the 72–88% of the pure cement's strength at 28 days and the 80–92% of the pure cement's strength at 90 days. It seems that the use of "0–5" fraction of slag improves the behaviour of the blended cements due to its higher fineness and higher content of hydraulic compounds, compared to the raw slag.

3.3. Cement hydration

Fig. 6 shows the X-ray diffraction patterns of cement with 15% steel slag hydrated for 1, 2, 7, 28 and 90 days. It can be seen that the main hydration products were C–S–H, $Ca(OH)_2$ and ettringite ($Ca_6Al_2(SO_4)_3{\cdot}32H_2O$) as well as unhydrated C_3S and C_2S. The peaks of the calcium silicates phases diminish, especially at the age of 90 days.

X-ray diffraction patterns (Fig. 7) of all cements hydrated for 28 days showed the formation of new products. Besides, $Ca_6Fe_2(SO_4)_3{\cdot}32H_2O$, FeO and FeO(OH) are also identified in samples with 30% and 45% steel slag. A part of wustite (FeO), presented in steel slag, seems to be transformed into FeO(OH) in the strong alkali environment of the hydrated cement pastes. Thereafter, $Ca_6Fe_2(SO_4)_3{\cdot}32H_2O$ starts to form, simultaneously with ettringite, with the consumption of FeO(OH) and sulphate while the combined water increases.

Fig. 8 shows the results of TGA of the hydrated cement pastes. The TG curves showed mass loss at about or around 130, 225, 500 and 825 °C, representing dehydration, dehydroxylation

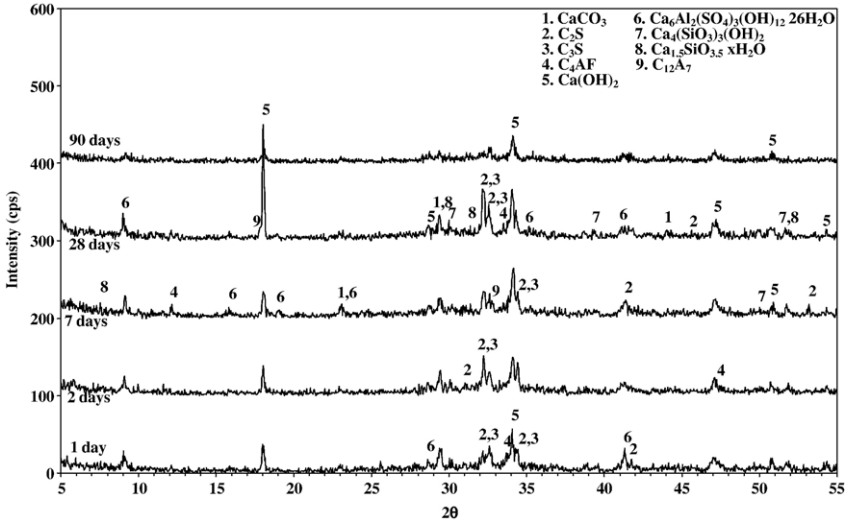

Fig. 6. X-ray diffraction of cement with 15% steel slag, hydrated at various ages.

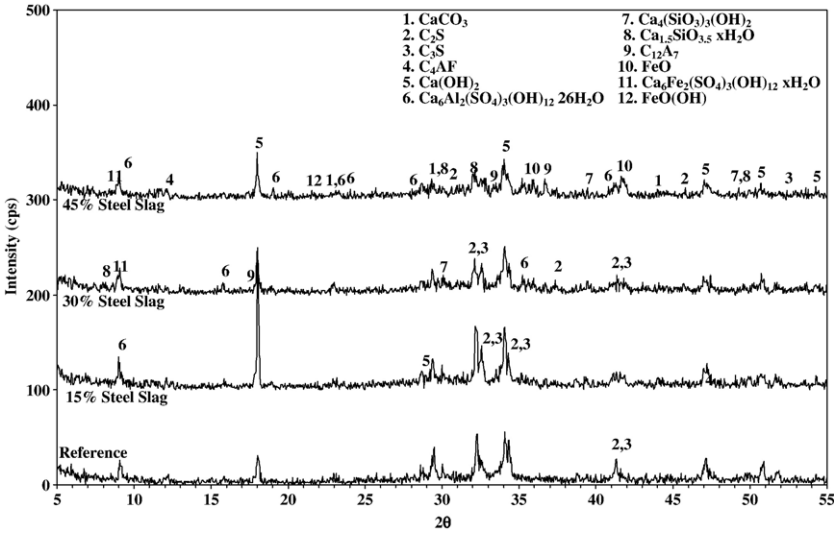

Fig. 7. X-ray diffraction of reference and blended cements, hydrated at 28 days.

or calcination of residual ettringite, decomposition of $Ca(OH)_2$ and decarbonation of calcium carbonate, respectively. In the 130–200 °C zone, the dehydration of the C–S–H gels takes place. It can be observed as a wide band that shifts to higher temperatures when the hydration age increases. This change takes place with a great mass loss. The second main mass loss can be observed at around 500 °C, which is attributed to the decomposition of crystalline $Ca(OH)_2$ produced by the hydration of calcium silicate phases of the blended cements. The data showed that $Ca(OH)_2$ content of the reference cement paste increased with the increase of the hydration age, whereas in the blended cements, there is a decrease with the hydration age, probably because of the steel slag hydration delay.

The non-evaporable water of the cement pastes, determined by TGA, is presented in Fig. 9. As it was expected, the non-evaporable water increases with hydration age (Fig. 9a). The

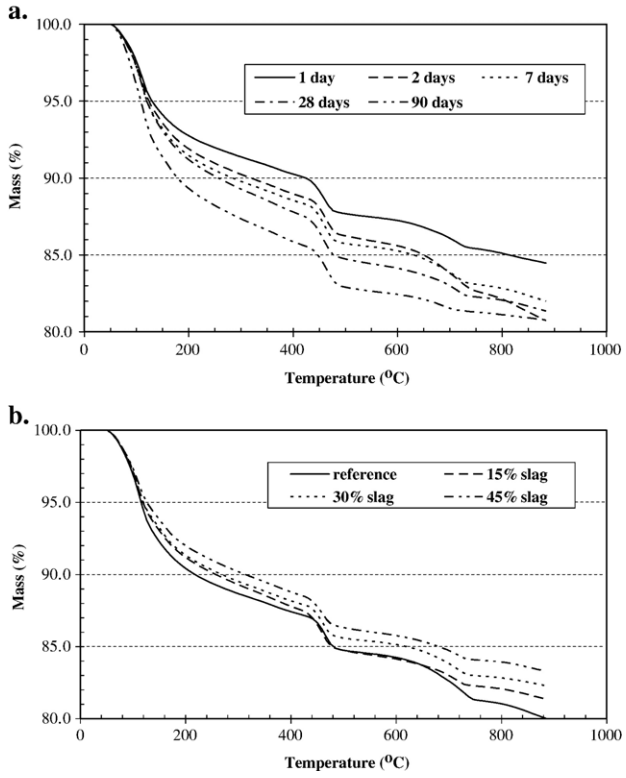

Fig. 8. TG diagrams (a: cement with 15% steel slag, hydrated at various ages, b: blended cements of various slag content, hydrated at 28 days).

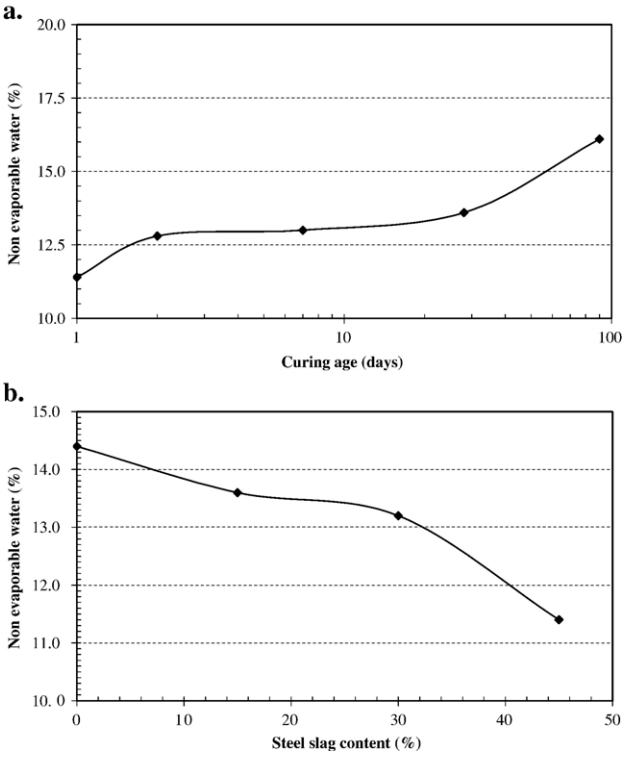

Fig. 9. Non-evaporable water (a: cement with 15% steel slag, hydrated at various ages, b: blended cements of various slag content, hydrated at 28 days).

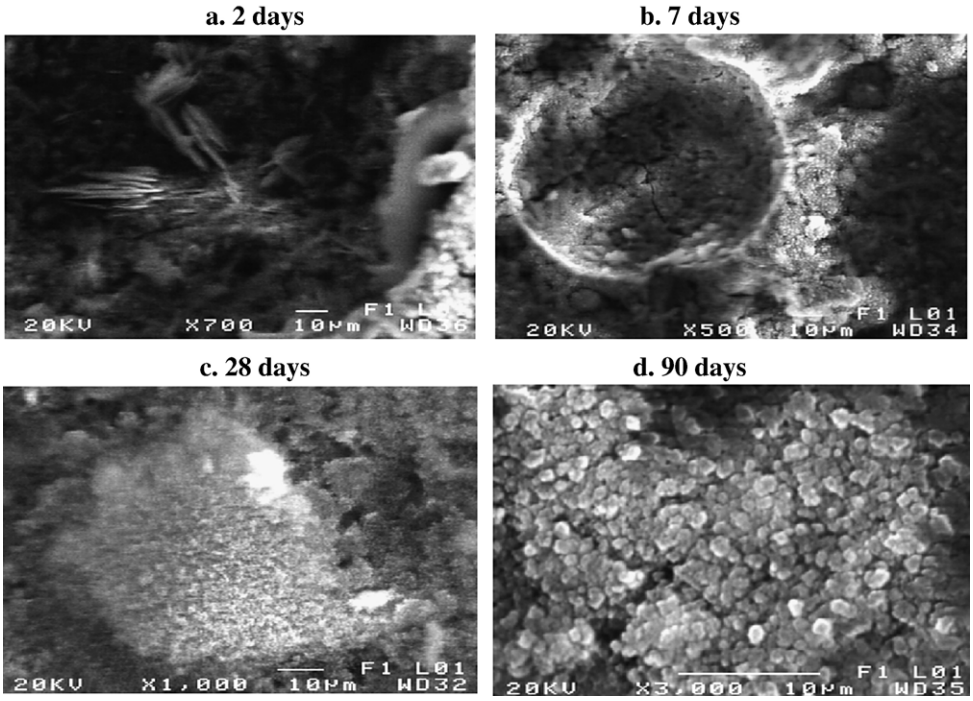

Fig. 10. SEM photos of cement pastes with 15% steel slag, hydrated at various ages.

increase of slag content leads to lower values of non-evaporable water due to the weak hydraulic activity of the steel slag used (Fig. 9b).

The typical microstructure (SEM) of fracture surfaces of cement pastes, at different curing ages, with or without slag incorporation are shown in Figs. 10 and 11. The typical morphology of hydrated cement was evident: a gel-like material surrounding cement grains. Although the changes are less visible, the reference sample as well as the cement containing 15% steel slag seems to be more compact, which is in accordance with the mechanical properties previously discussed. The C–S–H gel formed a dense network structure after 2 days. This showed that the hydration reaction of mixtures was fast enough and a lot of hydration products were formed. Thus,

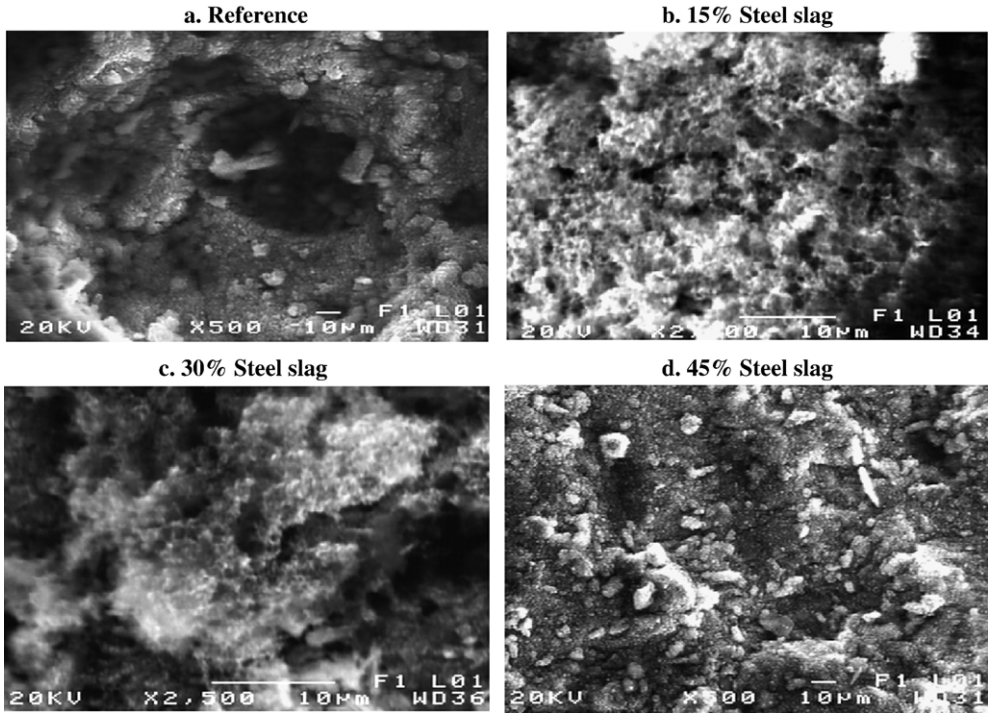

Fig. 11. SEM photos of blended cements, hydrated at 28 days.

the pastes structure tissue became dense. The micrograph of sample with 15% slag, at 2 days, shows small amount of crystallized needle-shaped ettringite inside pores (Fig. 10a). A high density of typical hexagonal plates of $Ca(OH)_2$ can be observed inside the capillary pores (Figs. 10b and 11a). The nature of the hexagonal crystals was determined by using Energy Dispersive Analysis (EDAX). Local concentrations of hydrated cement indicated the presence of anhydrous material, but with C–S–H hydration products forming a rim around steel slag (Fig. 10c). The C–S–H gel formed a fibrous network structure in cement pastes. As hydration progressed, other hydration products gradually filled the network structure (Fig. 11b and c). The cement paste structure became tight at the latter stage of hydration. At 90 days the surface became coarser, a fact that indicates the delayed reaction of steel slag (Fig. 10d). Furthermore, hydraulic reactions of slag mineral phases took place and their products filled the pastes pores. It should be noticed that in cases of 30% and, especially, 45% cement substitution, there are steel slag particles, at the later stages, which have only partially been hydrated. The EDAX analysis showed unreacted steel slag grains, which mainly contained iron and aluminum, with lesser amounts of calcium and silicon (Fig. 11d).

The XRD, TG and SEM observations confirm the fact that the rate of hydration in blended cements containing slag is lower than in pure PC. However, cements, containing up to 45 % steel slag, satisfy the requirements of the strength class 42.5 or 32.5 of EN 197-1. These cements have higher setting time and lower strength but they present certain advantages such as lower energy cost, higher abrasion resistance and lower hydration heat evolution and are suitable for mass concrete and pavement applications [1].

4. Conclusions

The following conclusions can be drawn from the study of the effect of steelmaking slag (size fraction: 0–5 mm) on the cement properties and hydration:

- Slag cements develop lower strength, at all ages, compared to the pure cement and the strength decrease is higher, the higher the slag content. In any case, cements containing 15% or 30% slag satisfy the requirements of the strength class 42.5 of EN 197-1, while the cements containing 45% slag satisfy the requirements of the strength class 32.5 of EN 197-1.
- The slag cements demand less water than the reference pure cement and the slag addition improves the mortar workability. On the contrary, the blended cements showed longer setting times than the pure one.
- The addition of steel slag slows down the hydration of the blended cements. This phenomenon was mainly attributed to the crystal size and structure of the C_2S contained in slag. It has a size more than 70 μm and it is characterized by clusters with finger structure with no well formed rounded crystals. This makes C_2S, known to react slowly, to react even slower.

References

[1] C. Shi, J. Qian, High performance cementing materials from industrial slags — a review, Resources, Conservation and Recycling 29 (3) (2000) 195–207.
[2] V.M. Malhotra, Properties of fresh and hardened concrete incorporating ground, granulated, blast furnace slag, in: V.M. Malhotra (Ed.), Supplementary Cementing Materials for Concrete, Minister of Supply and Services, Canada, 1987, pp. 291–336.
[3] B. Samet, M. Chaabouni, Characterization of the Tunisian blast-furnace slag and its application in the formulation of a cement, Cement and Concrete Research 34 (7) (2004) 1153–1159.
[4] S.J. Barnett, M.N. Soutsos, S.G. Millard, J.H. Bungey, Strength development of mortars containing ground granulated blast-furnace slag: effect of curing temperature and determination of apparent activation energies, Cement and Concrete Research 36 (3) (2006) 434–440.
[5] I. Teoreanu, A. Volceanov, S. Stoleriu, Non Portland cements and derived materials, Cement and Concrete Composites 27 (6) (2005) 650–660.
[6] A.R. Brough, A. Atkinson, Sodium silicate-based, alkali-activated slag mortars: part I. Strength, hydration and microstructure, Cement and Concrete Research 32 (6) (2002) 865–879.
[7] F. Collins, J.G. Sanjayan, Microcracking and strength development of alkali activated slag concrete, Cement and Concrete Composites 23 (4–5) (2001) 345–352.
[8] A. Altun, I. Yılmaz, Study on steel furnace slags with high MgO as additive in Portland cement, Cement and Concrete Research 32 (8) (2002) 1247–1249.
[9] H. Motz, J. Geiseler, Products of steel slags an opportunity to save natural resources, Waste Management 21 (3) (2001) 285–293.
[10] A. Monshi, M.K. Asgarani, Producing Portland cement from iron and steel slags and limestone, Cement and Concrete Research 29 (9) (1999) 1373–1377.
[11] C. Shi, S. Hu, Cementitious properties of ladle slag fines under autoclave curing conditions, Cement and Concrete Research 33 (11) (2003) 1851–1856.
[12] W. Xuequan, Z. Hong, H. Xinkai, L. Husen, Study on steel slag and fly ash composite Portland cement, Cement and Concrete Research 29 (7) (1999) 1103–1106.
[13] J.N. Murphy, T.R. Meadowcroft, P.V. Barr, Enhancement of the cementitious properties of steelmaking slag, Canadian Metallurgical Quarterly 36 (5) (1997) 315–331.
[14] L. Dongxue, F. Xinhua, W. Xuequan, T. Mingshu, Durability study of steel slag cement, Cement and Concrete Research 27 (7) (1997) 983–987.
[15] ASTM C204, Standard Test Method for Fineness of Hydraulic Cement by Air Permeability Apparatus, Document Number: ASTM C204-00, ASTM International (2000).
[16] E 196-3, Methods of testing cement — Determination of setting time and soundness (1994).
[17] ASTM C1437, Standard Test Method for Flow of Hydraulic Cement Mortar, Document Number: ASTM C1437-01, ASTM International (1999).
[18] ASTM C151, Standard Test Method for Autoclave Expansion of Portland Cement, Document Number: ASTM C151-00, ASTM International (2000).
[19] EN 196-1, Methods of testing cement — Determination of compressive strength (1994).
[20] A. Rai, J. Prabakar, C.B. Raju, R.K. Morchalle, Metallurgical slag as a component in blended cement, Construction and Building Materials 16 (8) (2002) 489–494.